

J. Environ. Treat. Tech. ISSN: 2309-1185

Journal web link: http://www.jett.dormaj.com https://doi.org/10.47277/JETT/9(3)685



Kinetic, Isotherm, and Thermodynamic Study of Methyl Orange Adsorption on Raw Clay from North of Morocco

Asmae LAAZIZ ¹, Imane KOUDA ^{1,2}, Abdeslam BARHOUN ¹, Khalid DRAOUI ^{1*}

¹ Laboratory of Materials and Interfacial Systems, Faculty of Sciences Tetouan, University Abdelmalek Essaadi-Morocco
² Laboratory of separation Process, Faculty of Sciences Kénitra University Ibn Tofail-Morocco

Received: 17/11/2020 Accepted: 19/06/2021 Published: 20/09/2021

Abstract

Clays and clay minerals have highly reactive surface and interesting texture properties that can easily remove organic and inorganic contaminants from wastewaters. In this perspective, this work reports the study of clay-pollutant interactions by using Moroccan clay as absorbents and methyl orange as an anionic model of dyes textile. The clay was sampled in the region of Tetouan. The Structural, and physicochemical properties of the sample were determined using different characterization techniques (XRD, FTIR, SEM, ATG/ADT, BET, and CEC). The results revealed that the raw clay is mainly composed of kaolinite and smectite as clay minerals. The SiO_2 / Al_2O_3 ratio was about 2.4. Its Cationic Exchange Capacity (CEC) was found to be 25.34 meq/100g. The specific surface area was equal to 51.28 m²/g. The adsorption isotherms were carried out using batch conditions. The kinetics adsorption of methyl orange (MO) on the clay revealed that equilibrium is rapidly reached. The data were adjusted by four kinetic models, including pseudo-first-order, pseudo-second-order, intra-particle diffusion model, and Elovich model. The pseudo-second-order model was the most adequate to describe the adsorption kinetics of the MO dye. The experimental results were modeled by four models, namely Langmuir, Freundlich, Dubinin Redushkevich (D-R), and Elovich. The adsorption isotherm showed that the Langmuir model perfectly represents the adsorption of methyl orange on the studied clay with a maximum adsorption capacity of 113 mg/g. The obtained thermodynamic parameters indicate that the adsorption of methyl orange is feasible and spontaneous. The obtained results showed clearly that the selected clay could be used as an adsorbent of anionic dyes.

Keywords: Clay, Methyl Orange, Characterization, Adsorption, Kinetic, Thermodynamic

1 Introduction

Over the last few years, environmental pollution has become a reality, which requires a deep reflection [1]. Industrials, scientists, and politicians are committed to developing and implementing the most efficient actions to limit its harmful effects [2]. Both human health and the environment can be seriously affected. Indeed, pollution impacts all the constituents of the environment: water, air, and soil. Particularly, water pollution is undoubtedly one of the most worrying aspects of the degradation of the natural environment [3]. The presence of micropollutants in water, even in infinitesimal amounts affects its quality, making it unsuitable for consumption and toxic for use [4]. Dyes are among these micropollutants intensively used in various industrial areas [5-6]. In the textile industry, there are more than 10, 000 dyes available with various and complex chemical structures [7]. Moreover, every year new products are brought on the market. These substances are highly soluble in water and can be in anionic, cationic, and non-ionic forms. To overcome the health problems caused by these dyes and to protect the environment, it is necessary to treat the residual effluents before it is discharged into the environment [8].

To face this environmental threat, many methods have been developed, such as coagulation/flocculation, photocatalysis, solvent extraction, evaporation, electrochemical oxidation, membrane separation, nanofiltration, advanced oxidation, and adsorption [9-11]. Among these techniques, the adsorption process has shown a high wastewater treatment capacity. It is very simple to implement and efficient for the removal of organic and inorganic pollutants. However, its high effectiveness is essentially related to its adsorbent nature, especially in terms of cost, availability, and regeneration. Many researchers have focused their interest on improving the adsorption capacities of raw solid materials. These include activated carbon [12-13] zeolites [14], layered double hydroxide materials [15], clays such as montmorillonite [16], bentonite [17] and kaolinite [18]. Clay minerals are generally phyllosilicates composed by the combination of the tetrahedral sheets based on silicon atoms and octahedral sheets often with aluminum as the central atom. Additionally, clay minerals can be found in fibrous morphology such as sepiolite and palygorskite. Isomorphic substitution in the tetrahedral and octahedral layers generates a permanent negative charge in the structure compensated by hydrated cations located in the interlamellar space [19]. The negative charge is located in the basal face. This charge is the key to the interaction with

^{*}Corresponding author: Khalid DRAOUI, Laboratory of Materials and Interfacial Systems, Faculty of Sciences Tetouan, University Abdelmalek Essaadi- Morocco; E-mail: khdraoui@gmail.com

different species. Furthermore, the edge face of clay minerals contains hydroxyl groups as active sites which are positively charged at acidic pH and negatively charged in an alkaline medium. Moreover, the state of the charge is highly dependent on the pHzc [20]. The efficiency of clays is particularly due to their capacity to retain both cationic and anionic compounds thanks to their lamellar structure, high CEC, swelling properties which provide interesting specific surface area [21] as well their texture and granulometry.

Clays can retain a significant number of harmful substances which gives great added value to these materials for use as water treatment or impermeable barriers in landfills. Several studies have focused on dyes' adsorption onto clays. The clayey soil may also be an alternative for the adsorption of pollutants. Its clay content may contribute to the retention of hazardous compounds. Based on what is cited above, we have selected a local clay sampled in the region of Saddena province of Tetouan (Morocco) as a low-cost alternative adsorbent for wastewater treatment. The Physico-chemical properties of the raw were evaluated by different techniques, such as X-ray diffraction (XRD), Fourier Transform Infrared Spectroscopy (FTIR), scanning electron microscopy (SEM/EDX), thermal analysis (TGA/DTG), specific surface area by BET method and cation exchange capacity (CEC) by the cobalthexamine method. The clay adsorption capacity of methyl orange MO in batch mode was evaluated by the determination of kinetic parameters and adsorption isotherm. The effect of pH and temperature was investigated to optimize the experimental conditions to remove MO from an aqueous medium.

2 Experimental

2.1. Materials

The studied clay was sampled from the natural basin Khemiss Anjra-Saddena located in the Tetouan region of northern Morocco. Before use, the raw material was dried 24 hours at 105° C, then crushed and sieved to obtain fractions of less than 200 μ m. The anionic dye Methyl Orange (MO) was purchased from Sigma-Aldrich and used without further purification. The MO stock solution was prepared by dissolving 1g of MO in 1 L of distilled water and stored in the dark at room temperature. The required concentrations were obtained by further dilution of the stock solution.

2.2. Characterization techniques

The mineralogical composition of the investigated clay was determined by using Bruker D8 Advance diffractometer operated with Cu-Kα radiation. The scanning speed was $0,016^{\circ}/s$ for 2θ angle ranged between 5 and 90° . The FTIR analysis was conducted using Spectrophotometer Thermo Vertex 70, in the range of 400-4000 cm⁻¹. The pellet press technique was adopted to improve the signal by mixing 1 mg of clay fine powder with 99 mg of KBr. The clay morphology was analyzed by scanning electron microscopy (SEM) (HIROX SH-4000M SEM) coupled with an EDS system from Brucker-AXS. The elemental composition was determined by an X-Ray fluorescence spectrometer (WDXRF, S4 Pioneer BRUKER) and the thermal stability by TA Instruments-Waters LLC, SDT Q600 analyzer. The heating rate was 5°C min⁻¹. Micomeritics Multi-point Beckman Coulter surface analyzer SA 3100 was used for texture characterization of the powder by adsorptiondesorption of Nitrogen at -196 °C. The specific surface area SSA was determined by the Brunauer-Emmet-Teller (BET) analysis. Cation exchange capacity was also evaluated using the cobalthexamine (Cl₃CO(NH₃)₆) method based on the variation of absorbance at 470 nm at the sample saturation. The concentrations of OM were determined using a UV-visible spectrophotometer of the type Jasco 630.

2.3. Adsorption experiments

The adsorption experiments were carried out in batch mode at room temperature. The adsorption isotherms were determined by the measurement of the variation of dye concentration. 100 mg of adsorbent was brought into contact with 20 mL of MO solution at different initial concentrations and stirred for 4 h. After equilibrium, the two phases have been separated by centrifugation at 3000 rpm for 15 min. The residual dye concentration was determined by the previously established calibration curve at the wavelength of 464 nm corresponding to the maximum MO absorbance. The adsorption capacity at the equilibrium is given by the following equation:

$$q_e = (C_0 - C_e) \frac{V}{m} \tag{1}$$

where, q_e (mg/g) corresponds to the amount of the adsorbed MO, C_o (mg/L) and C_e (mg/L) are the initial and equilibrium concentration of the dye, respectively, V (mL) is the volume of the solution, and m (g) the masse of the adsorbent.

3 Results and discussion

3.1. Clay characterization

3.1.1. Effect of pH

The determination of pH of the medium is required to quantify the contribution of surface acidity when the solid is in contact with the solution. For this purpose, 1 g of raw clay was dispersed in 100 ml of distilled water and stirred for 60 min with a magnetic stirrer at room temperature. The suspension is allowed to rest for 4h to reach the equilibrium. The pH was then measured using an electronic pH meter. The value found was about 5.66 revealings a low acidic character of the studied clay.

3.1.2. pH_{PZC} determination

The surface charge of materials depends strongly on the pH of the solution with which the material comes into contact. This charge can be positive, negative, or neutral depending on the medium conditions. An important characteristic of the surface is the point of zero charges (pH_{pzc}), which corresponds to the pH at which the net surface charge is neutral. It defines the acidity or alkalinity of the surface. At pH below pHpzc, the surface charge of the material is globally positive and at pH above pH_{pzc}, it is negative. This parameter is very important in sorption phenomena especially when electrostatic interactions are involved in the adsorption mechanism. The determination of the point of zero charges of the clay was conducted by batch method [22]. The variation of the pH between 1 and 12 was achieved by the addition of HCl (1N) and NaOH (1N) solutions. The clay suspension was maintained under agitation at 200 rpm for 24 hours to achieve equilibrium. The change in pH of each solution was measured and compared to the initial pH. The pH_{PZC} corresponds to the intercept point of the curve with the abscissa axis [23]. It was found to be 8.7 for the studied clay. The sample surface will get a negative charge over pH 8.7.

3.1.3. X-Ray Fluorescence analysis

Table 1 provides the elemental analysis of the clay sample carried out by XRF. It shows high clay mineral content reflected by the amount of alumina. The ratio SiO₂/Al₂O₃ is 2.4, related to the presence of 2:1 clay mineral [24-25]. It should be noted that the iron content is significant while the carbonate is low.

3.1.4. XRD analysis

The XRD technique was used to identify the minerals constituting the studied sample. The basal spaces were calculated by using the Bragg equation, $d = \lambda/2 \sin \theta$. Figure 2

shows that smectite (d_{001} = 12.8 Å) and kaolinite (d_{001} = 7.11 Å) are the main clay minerals in the raw clay [26-27]. The major associated mineral is quartz with an intense pic at 2 theta of 27° corresponding to (101) reflection plane.

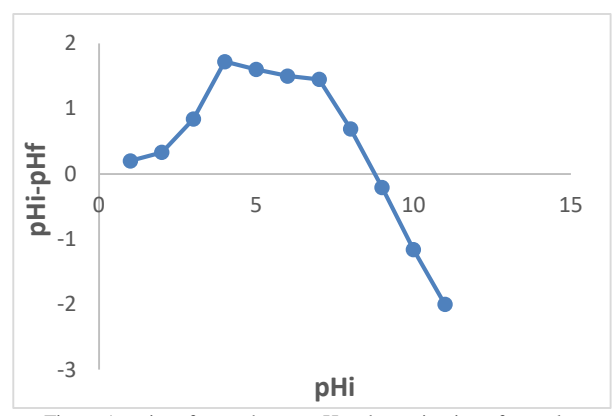


Figure 1: point of zero charges pH_{pzc} determination of raw clay

Table 1: XRF Elemental composition of the clay sample

Oxide	Composition %	
SiO_2	59.63	
Al_2O_3	24.86	
Fe_2O_3	11.37	
K_2O	1.58	
TiO_2	1.25	
CaO	1.14	
Cr_2O_3	0.053	
V_2O_5	0.05	
ZnO	0.022	
NiO	0.01	

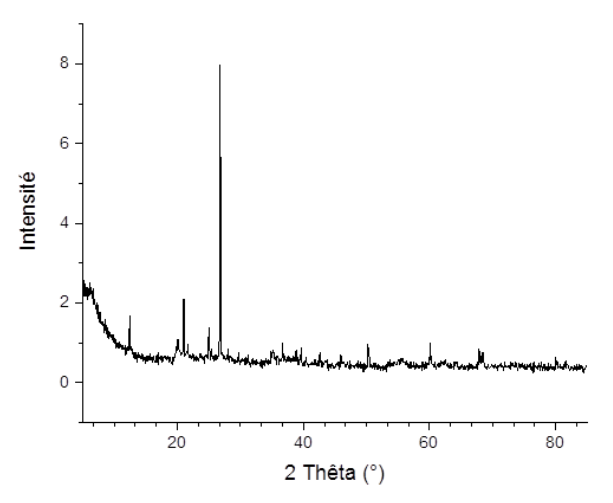


Figure 2: Powder XRD pattern of the clay sample

3.1.5. FTIR spectroscopy analysis

Infrared spectroscopy allows the identification of the clay surface groups [28]. The FTIR analysis of the studied clay is given in figure 3. The band at 3650 cm⁻¹ corresponds to stretching frequencies of kaolinite OH groups and the band located at 3625 cm⁻¹ is assigned to the Al–OH–Al stretching vibration of the smectite [29]. The bands at 3429 cm⁻¹ and 1630 cm⁻¹ are related to the stretching vibration and the bending mode of the water molecules that are associated with the exchangeable cations in interlayer spaces [30]. The bands in the

range 1120 cm⁻¹ and 1000 cm⁻¹ are due to the elongation vibrations of the Si-O bond, due to the presence of quartz and Si-OH, Al-OH and Al-O-Al groups of the clay minerals. The deformation vibration of the Al-Al-OH appears at 914 cm⁻¹ [31]. The bands around 500 cm⁻¹ and 400 cm⁻¹ may be attributed to deformation vibrations of the Al-O-Si bonds and deformation of the Si-O-Si linkages or elongation of the Fe-O bond, respectively. The bands at 2350-2320 cm⁻¹ are attributed to the asymmetric stretch mode of CO₂ [32].

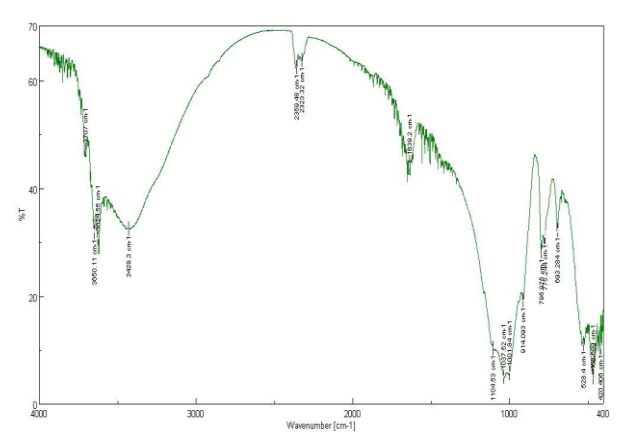


Figure 3: FTIR spectra of the clay sample

3.1.6. Scanning electron microscopy (SEM)

SEM was performed to examine the clay particles' morphology. The micrograph confirms that the material is composed of micrometric agglomerated particles. The morphology is irregular with an important porosity (Figure 4). EDS data are summarized in table 2. The results confirm those obtained by XRF. The clay contains mainly Si, Al, and Fe according to the presence of Al₂O₃, SiO₂, Fe₂O₃ (Table 2).

3.1.7. Thermal analysis

Thermal analysis was solicited to investigate the thermal stability of the clay sample. Three weight-loss events were observed in TGA/DTG thermograms with a total weight loss of 12.5% (Figure 5). The high value should be related to the presence of hydrated smectite. For the temperature below 300 °C, the weight loss is attributed to the release of physical and interfoliar water, respectively. The dehydroxylation of kaolinite is evidenced by the significant weight loss between 400 and 600 °C. This range is followed by a low mass loss due to dehydroxylation and a change in crystalline clay structure [34, 35].

Table 2: EDS elemental analysis of the clay

Element	Atomic %
0	63.03
Si	18.32
Al	11.23
Fe	3.17
K	0.65
Mg	0.99
C	1.55
Ca	0.44
Na	0.62

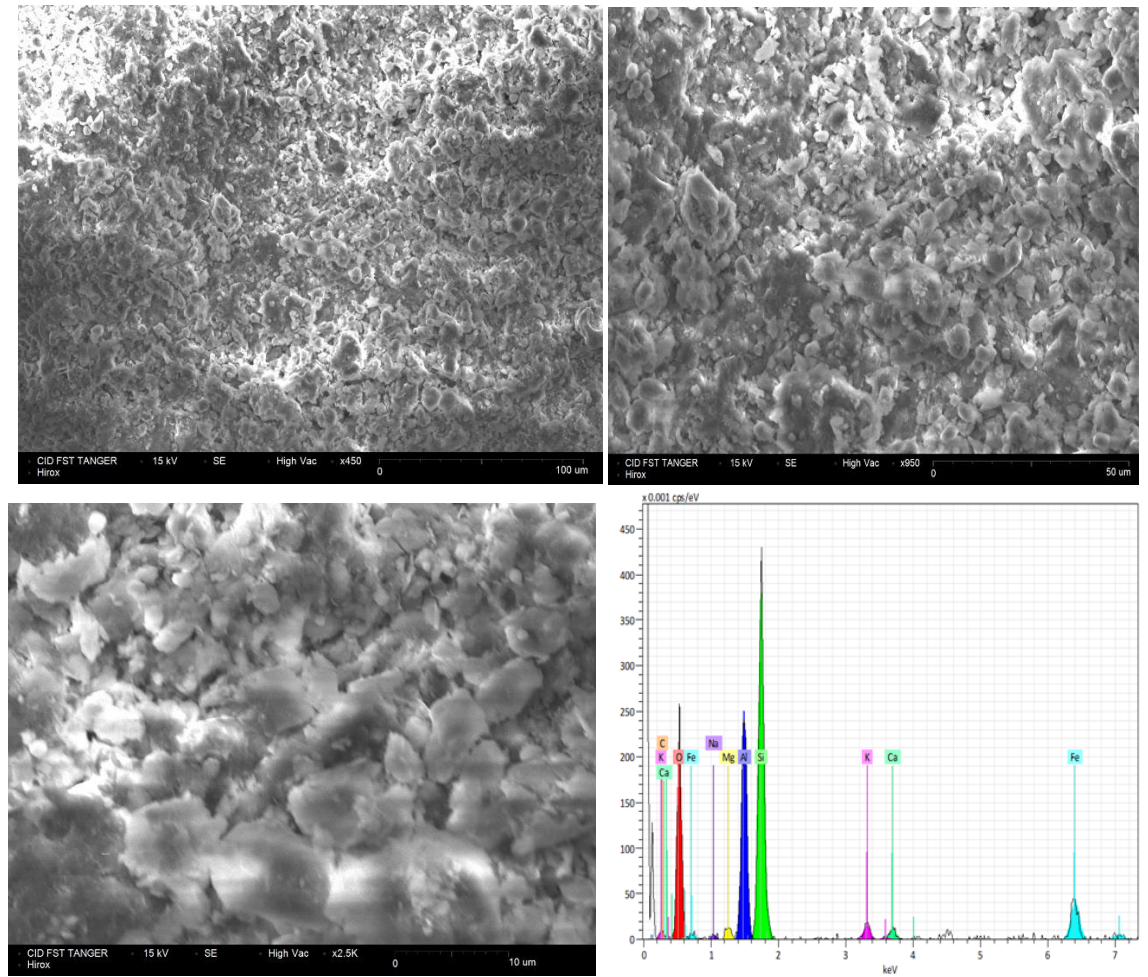


Figure 4: SEM images of clay sample and EDS analysis

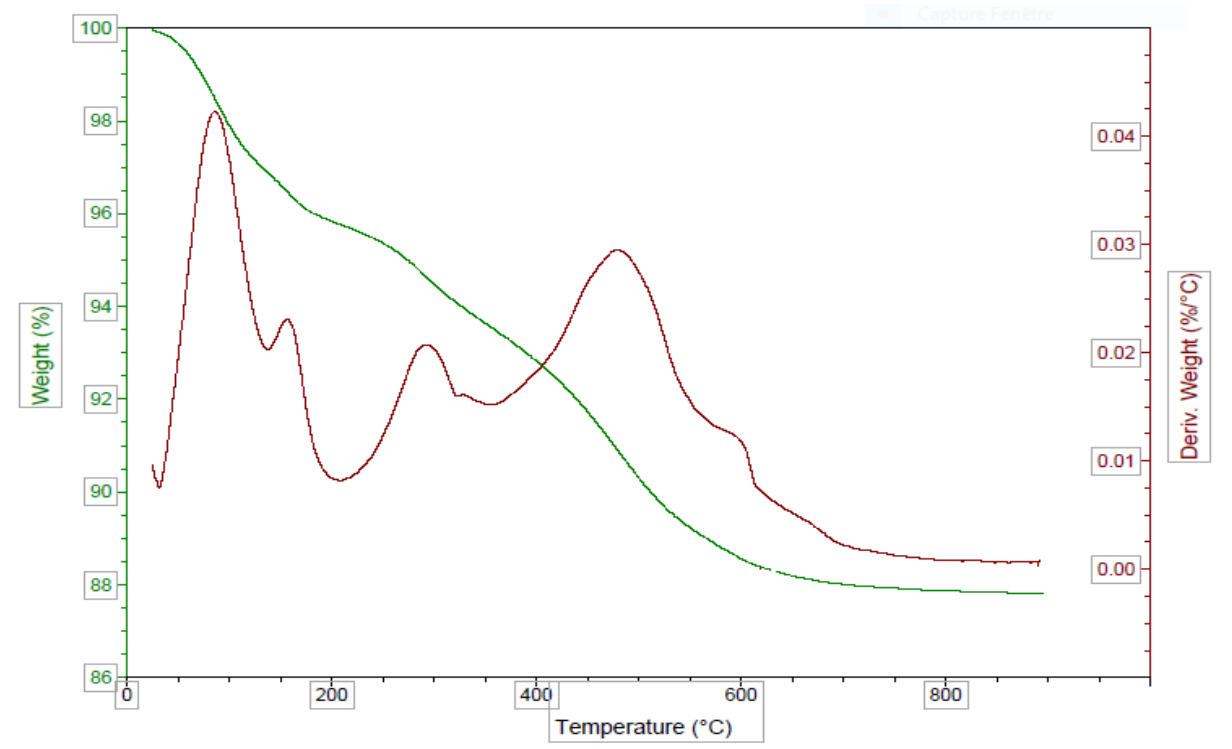


Figure 5: TGA/DTG thermograms of the clay sample

3.1.8. Specific surface area

Textural characterization of the clay was performed by nitrogen adsorption-desorption volumetry. The specific surface area was estimated using the BET model [36] at the linear part. The molecular area of N_2 is about $0.162~\text{nm}^2$. Figure 6 shows that the adsorption-desorption isotherm belongs to type IV, characteristic of mesoporous solids due to the presence of hysteresis loop of H4 in the P/P0 range of 0.45 to 0.95 [37]. The value of the specific surface area S_{BET} is about 51.28 m^2/g which is close to that found for smectites.

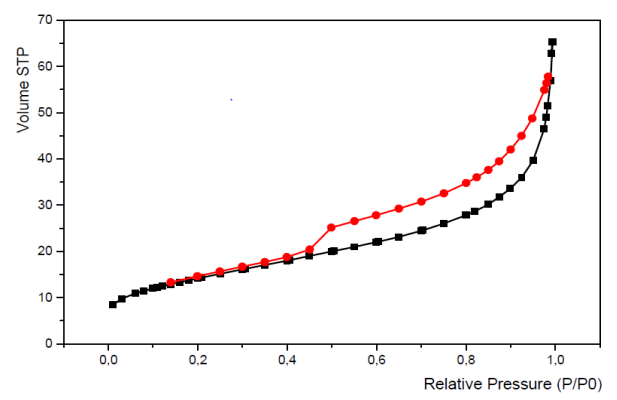


Figure 6: Nitrogen adsorption and desorption curves of clay sample

3.1.7. Cation exchange capacity (CEC)

Cation exchange capacity (CEC) is the total capacity of materials to retain exchangeable cations which measurement is important since it allows the prediction of the adsorption mechanism of cationic molecules. There are several methods for the determination of CEC. In this work, the standard cobalthexamine method was used [38]. The cation exchange capacity of the analyzed clay sample is approximately 25.34 meq/100g. This value is within the range corresponding to the presence of swelling clay, which is in agreement with the X-ray diffraction results.

3.2. Adsorption study

3.2.1. Adsorption kinetic

Adsorption kinetics, expressed in terms of the quantity of solute retained as a function of contact time, is one of the defining characteristics of adsorption efficiency [39]. The Effect of time on adsorption exhibits two distinct stages as shown in figure 7. During the first hour, the adsorption capacity increases rapidly. This can be explained by the high availability of adsorption sites and the strong interaction at the dye/adsorbent interface. In the second step, adsorption capacity increases slightly until reaching equilibrium. The kinetic data were modeled using the four most commonly used equations to characterize the adsorption mechanism: pseudo-first-order, pseudo-second-order, intra-particle diffusion, and Elovich. The pseudo-first-order model is the oldest kinetic model, proposed by Lagergren [40], according to the following equation:

$$log(q_e - q_t) = logq_e - \frac{k_1}{2.303}t$$
 (2)

where t is the contact time, q_t and q_e (mg/g) are the amounts adsorbed at time t and equilibrium respectively, k_1 is the pseudo-first-order rate kinetic (min^{-1}) . Figure 8 shows clearly that this model is not adequate to describe the kinetic data. This result is supported by a very low correlation coefficient and a large difference between the values of the theoretical and experimental adsorption capacities (Table 3).

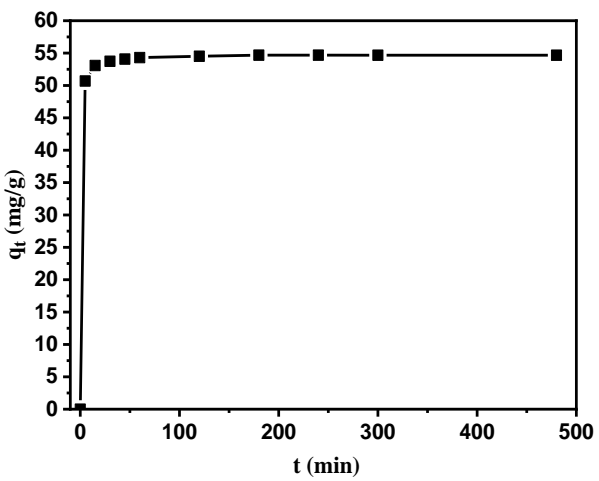


Figure 7: Kinetic adsorption of MO on raw clay, [MO]= 400 mg/L

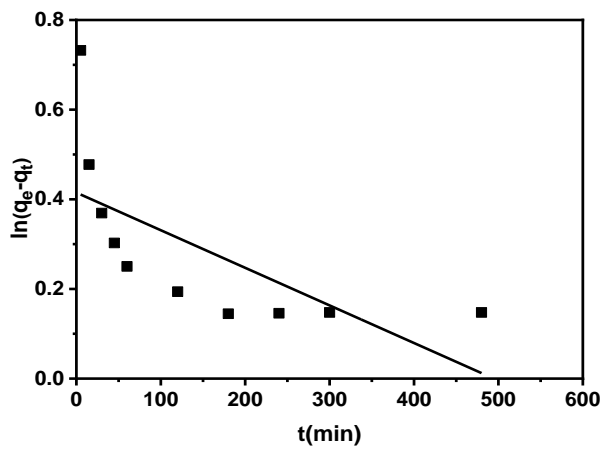


Figure 8: Pseudo-first-order plot of MO adsorption on clay sample

The kinetic model of pseudo-second-order indicates that the mechanism is chemisorption which considers the fast fixation of the adsorbate on the most reactive sites and that of a slow fixation on the sites of less energy [41-42]. The model is expressed by:

$$\frac{t}{Q_{t}} = \frac{1}{k_{2}qQ_{e}^{2}} + \frac{1}{Q_{e}}t\tag{3}$$

where k_2 is the pseudo-second-order rate constant (min⁻¹). Figure 9 shows the result of the experimental data modeling of this kinetic model. The linearity of the curve is noticeable, and the correlation coefficient is equal to 1 as illustrated in Table 3. Moreover, the calculated value of $q_{e,cal}$ (54.64 mg.g⁻¹) is comparable to the experimental value. Therefore, the MO adsorption process on the investigated clay is governed by a chemisorption mechanism. Several studies have also reported that the adsorption of dyes on some clay substrates from an aqueous medium follows the pseudo-second-order model [43-45]. The intra-particle diffusion model is generally applied to identify the rate-limiting step of the retention process since other models do not specify the diffusion mechanism. It was proposed by Weber and Morris [46] and presented by the following equation:

$$q_t = k_i t^{\frac{1}{2}} + C \tag{4}$$

where k_i (mg/g.min^{1/2}) is the intra-particle diffusion rate constant and C (mg/g) is the constant indicating the thickness of the boundary layer. These constants can be experimentally

determined from the slope and intercept at the origin by plotting the curve K_i as a function of $t_{1/2}$ (Figure 10).

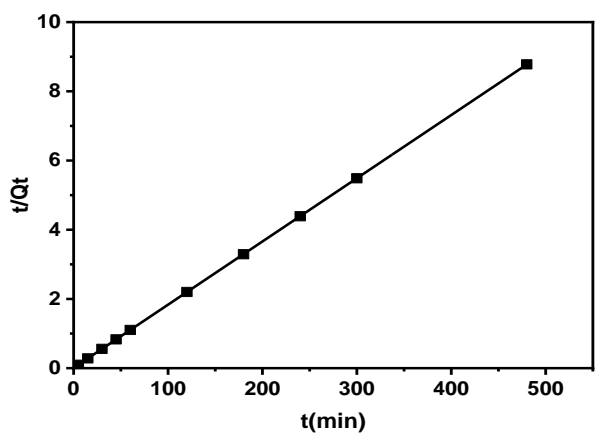


Figure 9: Pseudo-second-order plot of MO adsorption on clay sample

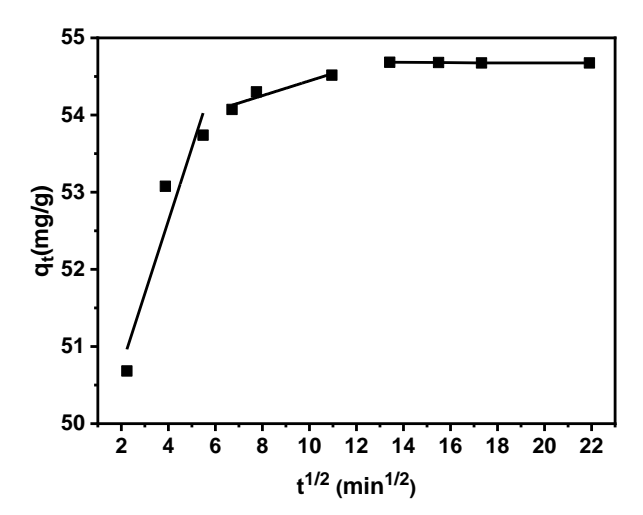


Figure 10: Intra-particle diffusion plot of MO adsorption on clay sample

As shown in figure 10, the experimental data are divided into three steps. The first stage of the plot characterized by a relatively high slope is allocated to external diffusion allowing MO molecules to reach the external surface of the clay. This step has the highest value of the intra-particle diffusion rate constant. (Table 3). Then the adsorbate diffuses from the

external surface to the adsorption site in the porous structure which corresponds to intraparticle-diffusion. The third stage reflects adsorption accompanied by a decrease in MO concentration until reaching equilibrium. Table 3 shows that the correlation coefficient is high for the three stages, thus it seems that this model perfectly represents the obtained data. Moreover, the values of the intercept (C) increase as a function of time, indicating that the effects of external mass transfer resistance become progressively higher. Indeed, an increase in the value of C indicates the abundance of solute adsorbed on the boundary layer [47]. Otherwise, the Elovich model is also used to represent the chemisorption on the heterogeneous surface [48]. The equation is formulated as follow:

$$\frac{q_t}{at} = \alpha e^{(-\beta q_t)} \tag{5}$$

where α (mg/g.min) is the adsorption initial rate, β is a constant that represents the extent of surface coverage and chemisorption activation energy. Elovich equation can be simplified, by assuming that $\alpha\beta t >> 1$ [49]. The following equation is then obtained:

$$q_t = \frac{1}{\beta} \ln(\alpha \beta) + \frac{1}{\beta} \ln t \tag{6}$$

The constants α and β are determined by plotting q_t versus lnt as shown in Figure 11. Based on the low value of the correlation coefficient (Table 3), the Elovich equation is not suitable to predict the adsorption mechanism.

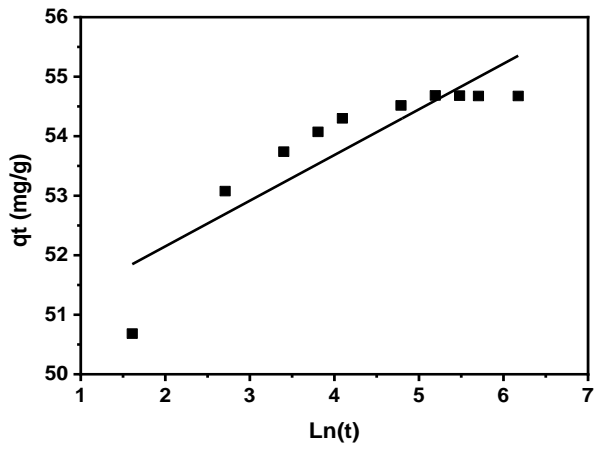


Figure 11: Elovich model plot of MO adsorption on clay sample

Table 3: Kinetic parameters of MO adsorption on clay sample

Kinetic model	Parameter	Value	\mathbb{R}^2
Qe experimental	qe _(exp) (mg/g)	55.52	
Pseudo-first order	K_1 (min ⁻¹)	0.002	0.46
	q_{calc} (mg/g)	1.51	0.40
Pseudo-second order	$K_2(g/(mg.min))$	0.04	1
	q_{calc} (mg/g)	54.64	1
	$Ki_1 (mg/(g.min^{1/2})$	0.94	0.01
Intra-particular diffusion	$C_1 (mg/g)$	48.85	0.91
	$K_{i2} (mg/(g.min^{1/2}))$	0.10	0.01
	$C_2 (mg/g)$	53.48	0.91
	$K_{i3} (mg/(g.min^{1/2})$	0.001	0.72
	$C_3 (mg/g)$	54.70	0.73
Elovich	α (mg/g.min)	7.28E+06	0.77
	β (g/mg)	2.995	0.77

3.2.2 pH Effect

the pH of the medium is an essential parameter to consider in adsorption processes. This parameter affects both the solubility and the ionization state of the sorbate. It significantly affects the mobility of ions [50,51]. The adsorbent surface charge is also closely related to this parameter. The influence of pH on the MO adsorption onto the studied material was examined for values ranging from 2 to 12. For this purpose, 100 mg of adsorbent was introduced into 25 mL of MO solution, keeping contact time to 4h, stirring speed of 200 rpm at room temperature. Acidification and alkalization of the solutions were carried out by adding 1N HCl or 1N NaOH solutions. The results are shown in figure 12.

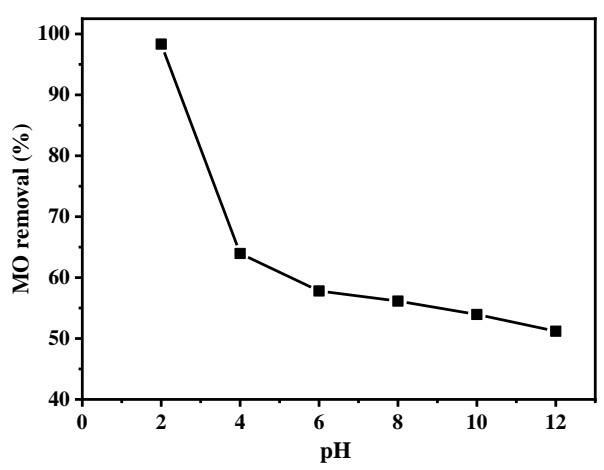


Figure 12: Effect of pH on the adsorption of MO on clay sample

The adsorption capacity is highest at acidic pH and decreases significantly (about 40%) between pH 2 and 4. Above pH 4, the percentage of OM removal is slightly reduced. In an acidic environment, the surface of the adsorbent becomes more positively charged improving the attraction of the anionic dye molecules. In an alkaline medium, hydroxyl anions compete with the OM, contributing to a decrease in its adsorption. A similar result was reported by Jalil et al. [44]

3.2.3 Adsorption isotherm and temperature effect

The adsorption isotherm is a simple and useful tool to specify the affinity between the adsorbent and the adsorbate. It allows determining the effective variation of the adsorbed quantities according to the concentration often expressed at equilibrium. The adsorption capacity is directly linked to the temperature which may affect the adsorption process [9,10]. Moreover, it is interesting to investigate this parameter since several industrial effluents are discharged into the environment at high temperatures. The evolution of the adsorption capacity was conducted at different initial concentrations and temperatures. Figure 13 shows that the temperature induces to a decrease in the adsorption capacity of the studied clay. The adsorption process must be exothermic, which favors the desorption process in the sorption mechanism. Similar findings were cited by Yu and Luo [52], for the adsorption of the MO dye on mesoporous activated carbon. Several theoretical models have been developed to describe the adsorption isotherms. In this study, four models were applied, including Langmuir, Freundlich, D-R, and Temkin to better understand the adsorption process.

Langmuir model:

The Langmuir adsorption isotherm assumes that the adsorbent has a fixed and equivalent number of adsorption sites

[53]. The species should be compacted as a monolayer surface without any lateral interaction between adsorbed molecules. The linear form of the Langmuir isothermal model is expressed by the following equation:

$$\frac{1}{q_e} = \frac{1}{q_{max}} + \frac{1}{q_{max}k_L} \frac{1}{C_e} \tag{7}$$

where qe (mg/g) is the adsorption capacity at the equilibrium, q_{max} is the maximum adsorption capacity (mg/g) which corresponds to the complete formation of the monolayer, C_e (mg/L) is the MO equilibrium concentration and K_L (L/mg) is the Langmuir isotherm constant related to the affinity of the surface sites for the adsorbate. q_{max} and k_L were determined by plotting $1/q_e$ versus $1/C_e$ (Figure 14)

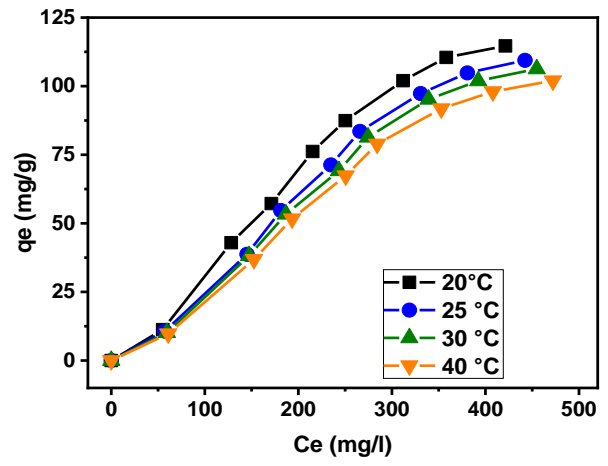


Figure 13: Adsorption isotherms and effect of temperature on the MO adsorption

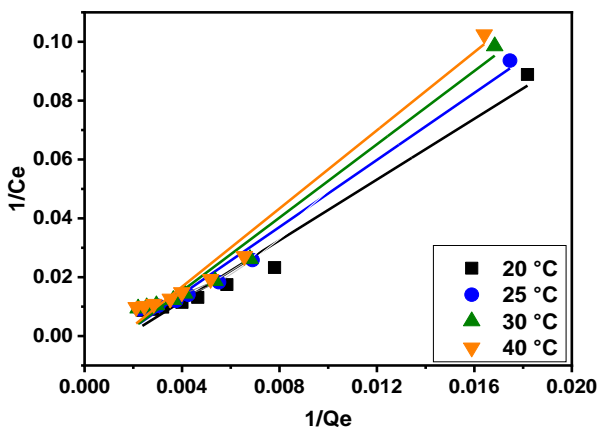


Figure 14: Langmuir isotherm plots for MO adsorption on Clay

The essential characteristics of the Langmuir isotherm can be expressed by the dimensionless parameter known as the separation factor or equilibrium parameter, R_L, which is expressed as

$$R_L = \frac{1}{1 + k_L C_0} \tag{8}$$

where C_0 is the initial concentration. The Langmuir model parameters, presented in Table 4, are reasonable to describe the adsorption process of MO on studied clay. The correlation coefficients are all close to 1, and the q_{max} values calculated from the Langmuir equation are comparable to those obtained experimentally. The R_L values obtained for all temperatures are

between 0 and 1, indicating that the adsorption process of MO on the clay is favorable.

Freundlich model

Freundlich model is an empirical isotherm based on adsorption on heterogeneous surfaces [54]. The adsorption sites are considered not equivalent; therefore, the adsorption takes place first on the most active sites. The Freundlich equation is expressed by:

$$q_e = k_f C_e^{\frac{1}{n}} \tag{9}$$

The equation can be linearized as follows:

$$lnq_e = logk_f + \frac{1}{n_f} lnC_e \tag{10}$$

where k_f and n_f are the Freundlich constants, n_f expresses the adsorption strength, k_f and n_f were determined by the plot of lnq_e variation with lnC_e (Figure 15). The intercept with the x-axis corresponds to lng_f while the slope is equal to 1/n value.

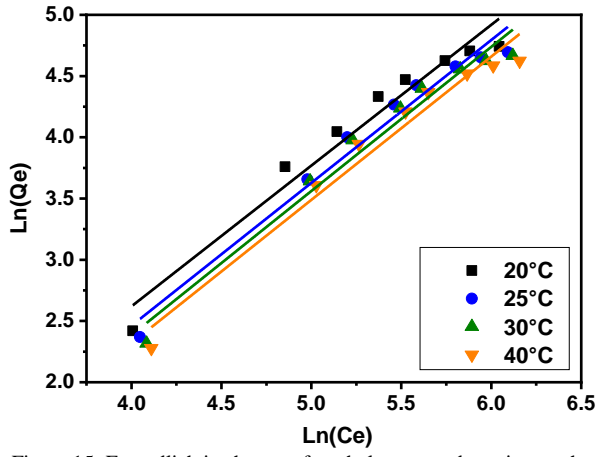


Figure 15: Freundlich isotherms of methyl orange adsorption on the clay

The adsorption isotherm exhibits an acceptable fitting for the studied temperatures. The correlation coefficient is also higher but slightly low than those obtained by the Langmuir model (Table 4). The acceptable fit of experimental data by the Freundlich equation is probably because the monolayer was not saturated. $k_{\rm f}$ values increase with increasing temperature according to the improvement of adsorption capacity. The parameter 1/n is lower than 1, adsorption is therefore quite favorable.

Dubinin-Radushkevich (D-R) model

The Dubinin-Radushkevich model is based on adsorbent porosity and adsorption energy [55]. It provides insight into the adsorption mechanism and the possibility to distinguish between physical and chemical adsorption. The model is expressed as follows:

$$q_e = q_{max} e^{(-K_{DR}\varepsilon^2)}$$
(11)

The equation can be linearized as:

$$lnq_e = lnq_{max} - K_{DR}\varepsilon^2$$
 (12)

in which, q_{max} (mg/g) is the maximum theoretical capacity of adsorption, ϵ is the Polanyi potential. K_{DR} (mol²/kJ²) is related to the adsorption free energy, given by:

$$\varepsilon = RT \ln \left(1 + \frac{1}{c_{\star}} \right) \tag{13}$$

 K_{DR} and E (kJ/mol) are linked by the following equation [56]:

$$E = (2K_{DR})^{-0.5} (14)$$

By plotting lnq_e versus ϵ^2 , the value of q_{max} , K_{DR} and E could be calculated (Figure 16).

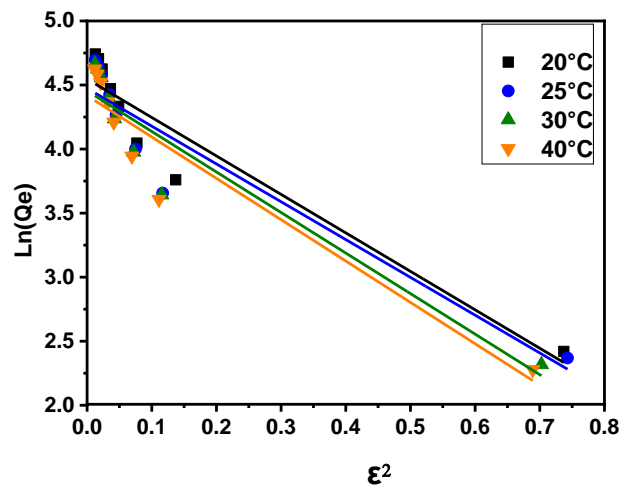


Figure 16: Dubinin-Radushkevich isotherms of methyl orange adsorption on the clay

The energy (E) calculated from the D-R isotherm gives useful information on the properties of the physical or chemical adsorption process [57]. $K_{\rm DR}$ values are in the same order of magnitude (Table 4). The maximum adsorption capacity is not under the experimental data and the correlation coefficient is low, therefore this model is not suitable to describe the adsorption isotherm data.

Temkin model

The Temkin model used by Hayward and Trapnell assumes that the affinity decreases linearly not logarithmically with increasing adsorption on the surface of the material [58,59]. The Temkin isotherm is generally expressed by the following equation:

$$q_e = Bln(K_T C_e) \tag{15}$$

The linear form of the equation is as follows:

$$q_e = BlnK_T + BlnC_e \tag{16}$$

where B is equal to $\frac{RT}{b_T}$, K_T (L/g) is the equilibrium binding constant, B (J/mol) is the Temkin constant related to the adsorption heat, R is the universal gas constant (8.314 J/mol. K), and T is temperature. The plot of q_e variation with lnC_e is used to determine B and K_T (Figure 17). The parameters of the Temkin equation are given in Table 4. The modeling of the experimental data shows that the Temkin constant (B) decreases with temperature, indicating that adsorption is exothermic, which confirms our experimental results. The correlation coefficients are high (≥ 0.97), suggesting that it is possible to implement this model for the description of experimental data.

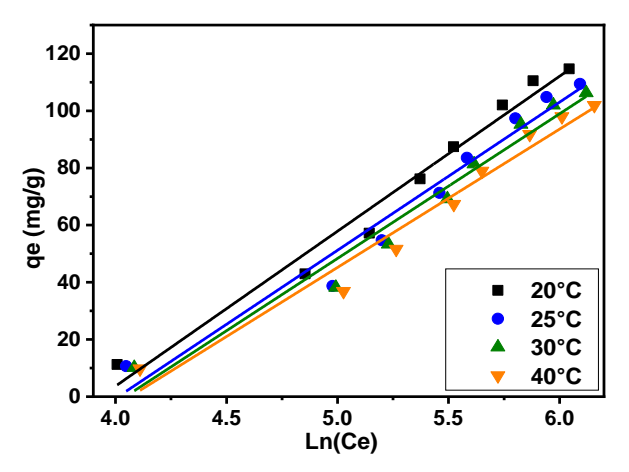


Figure 17: Temkin isotherms of MO adsorption on the clay sample

3.2.4 Thermodynamic study

The thermodynamic study provides information on the spontaneity of the adsorption process [60]. Several researchers focused on the determination of parameters such as free energy (ΔG°) , enthalpy (ΔH°) and entropy (ΔS°) variations estimated from equilibrium constants at different temperatures. The free energy variation of the adsorption reaction is given by the Van't Hoff equations:

$$\Delta G^o = -RT ln K_c \quad (17)$$

$$lnK_c = -\frac{\Delta H^o}{RT} + \frac{\Delta S^o}{R}$$
 (18)

where ΔG° is the Gibbs free energy change (kJ/mol), ΔH° is the enthalpy variation (kJ/mol) and ΔS° is the entropy change (J/K.mol), K_c is equilibrium adsorption constant (L/mg). ΔH° and ΔS° are deduced from Figure 18.

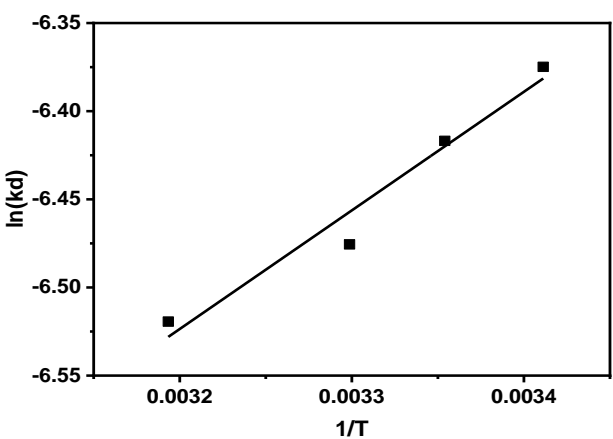


Figure 18: Van't Hoff representation for the MO adsorption on the clay sample

The thermodynamic parameters of adsorption were determined from the experimental data obtained at different temperatures. The values of ΔG are all negative, which reflects the spontaneous behavior of the adsorption process (Table 5). The negative values of ΔH confirm the exothermic nature of the above process.

4 Conclusion

This study focused on the evaluation of the effectiveness of raw Moroccan clay from the Tetouan region to remove the methyl orange, as an anionic model dye, from an aqueous medium. The characterization revealed that kaolinite and smectite are the two main clay minerals composing this natural material. This raw material is also relatively rich in iron and presents an interesting specific surface area and cation exchange capacity. The adsorption performance depends on the pH of the solution with high adsorption of dye at an acidic medium. The kinetic study showed that equilibrium is rapid and established after 60 minutes of contact time. The adsorption mechanism can be described by pseudo-second-order kinetics. Besides, the clay has shown high efficiency in removing MO anionic dye with a maximum adsorption capacity of 113 mg/g.

Table 4: Adsorption parameters according to the models of Langmuir, Freundlich, Temkin and D-R

Isotherm model	Domomotoms	Temperature (K)			
Isomeriii iiiodei	Parameters	293	298	303	313
	q _{max} (mg/g)	113.64	108.70	104.17	102.04
Langmuir	K_L (L/mg)	0.002	0.002	0.002	0.001
_	\mathbb{R}^2	0.99	0.99	0.98	0.98
	$ m K_{f}$	7.23	8.35	10.20	10.60
Freundlich	\mathbf{n}_{f}	0.87	0.87	0.85	0.90
	\mathbb{R}^2	0.97	0.97	0.96	0.96
Temkin	K_T (L/mg)	51.02	55.24	57.07	58.29
	B (kJ/mol)	54.21	51.81	50.60	48.38
	\mathbb{R}^2	0.98	0.98	0.97	0.97
	$\mathbf{q}_{\mathbf{max}} (\mathbf{mg/g})$	94.34	87.71	85.98	82.86
D-R	$\mathbf{K}_{\mathbf{D}\mathbf{R}} (\text{mol}^2/\text{kJ}^2)$	3.00	2.86	3.16	3.23
	E (kJ/mol)	0.39	0.42	0.40	0.39
	\mathbb{R}^2	0.92	0.90	0.90	0.90
	\mathbb{R}^2	0.75	0.86	0.82	0.83

Table 5: Thermodynamic Parameters of MO adsorption on clay sample

Te	emperature (K)	$\Delta \mathbf{G}^{\circ}$ (kJ/mol)	Δ H $^{\circ}$ (kJ/mol)	$\Delta \mathbf{S}^{\circ} (\mathbf{J/mol.k})$
·	293	-5.449	-5.47	
	298	-5.448		-0.072
	303	-5.448		-0.072
	313	-5.447		

The adsorption isotherms were successfully fitted by the Langmuir model. Moreover, the increase in temperature leads to a decrease in the adsorption capacity. The obtained thermodynamic parameters indicate that the adsorption of the methyl orange dye is exothermic, physical, and spontaneous in nature. The abundance of this natural material in the Tetouan region may therefore offer a low-cost alternative for the treatment of wastewater effluents with a view to their reuse in irrigation of green spaces or to dedicate these lands as an impermeable area for the implementation of a landfill site.

Acknowledgment

This work was financially supported by CNRST-Maroc (Projets dans les domaines prioritaires de la Recherche Scientifique et du développement technologique PPR2)

Ethical issue

Authors are aware of and comply with, best practices in publication ethics specifically about authorship (avoidance of guest authorship), dual submission, manipulation of figures, competing interests, and compliance with policies on research ethics. Authors adhere to publication requirements that submitted work is original and has not been published elsewhere in any language.

Authors' contribution

Asmae LAAZIZ: Conceptualization, Methodology, Characterization Investigation, Data Analysis.

Imane KOUDA: Methodology, Data Analysis.

Abdeslam BARHOUN: Conceptualization, Data Analysis, Review

Khalid DRAOUI: Supervision, Resources, Conceptualization, Methodology, Data Analysis, Writing -review & editing,

Competing interests

The authors declare that they have no known competing financial interests or personal relationships that could have appeared to influence the work reported in this paper

References

- [1] Ting L., Tao X., Xue-Lian H., Cheng L., Wei-Feng Z., Qian Z., Chang-Sheng Z., Post-crosslinking towards stimuli-responsive sodium alginate beads for the removal of dye and heavy metals, Carbohydr. Polym. 2015, 133:587–595. https://doi.org/10.1016/j.carbpol.2015.07.048
- [2] Ngulube T., Jabulani R,G, Vhahangwele M., Arjun M., An update on synthetic dyes adsorption onto clay based minerals: A state-ofart review, J. Environ. Manage. 2017, 191:35-57. <u>DOI:</u> 10.1016/j.jenvman.2016.12.031
- [3] Ahmad A., Rafatullah M., Sulaiman O., Ibrahim M.H., Hashim R., Scavenging behaviour of meranti sawdust in the removal of methylene blue from aqueous solutionJ. Hazard. Mater. 2009, 170:357–365. DOI: 10.1016/j.jhazmat.2009.04.087.
- [4] Zhang W., Yan H., Li H., Jiang Z., Dong L., Kan X., Yang H., Li A., Cheng R., Removal of dyes from aqueous solutions by straw based adsorbents: batch and column studies. Chem. Eng. J., 2011, 168:1120–1127. https://doi.org/10.1016/j.cej.2011.01.094
- [5] Annadurai G., Ling L.Y., Lee J.F., Adsorption of reactive dye from an aqueous solution by chitosan: isotherm, kinetic and thermodynamic analysis, J. Hazard. Mater. 2008, 152:337– 346. DOI: 10.1016/j.jhazmat.2007.07.002
- [6] Kausar A., Iqbal M., Javed A., Aftab K., Nazli Z. H, Bhatti H. N., Nouren S., Dyes adsorption using clay and modified clay: A review, J. Mol. Liq. 2018, 256:395–407. DOI: 10.1016/j.molliq.2018.02.034
- [7] Hassaan M. A., El Nemr A., Health and Environmental Impacts of Dyes: Mini Review Am. J. Environ. Sci. Eng., 2017, 1:64-67. <u>DOI:</u> 10.11648/j.ajese.20170103.11

- [8] Kehrein P., Loosdrecht M. V., Osseweijer P., Garfí M., Dewulf J., Posada J., A critical review of resource recovery from municipal wastewater treatment plants: market supply potentials, technologies and bottlenecks Environ. Sci.: Water Res. Technol., 2020, 6:877-910. https://doi.org/10.1039/C9EW00905A
- [9] Ahrouch M., Gatica J., Draoui K., Bellido D., Vidal H., Lead removal from aqueous solution by means of integral natural clays honeycomb monoliths, J. Hazard. Mater., 2019, 365:519-530. DOI: 10.1016/j.jhazmat.2018.11.037
- [10] Bentahar Y., Hurel C., Draoui K., Khairoun S., Marmier N., Adsorptive properties of Moroccan clays for the removal of arsenic (V) from aqueous solution, Appl. Clay Sci., 2016, 119:385–392. https://doi.org/10.1016/j.clay.2015.11.008
- [11] Crini G., Badot P.M., Application of Chitosan, a Natural Aminopolysaccharide, for Dye Removal from Aqueous Solutions by Adsorption Processes Using Batch Studies: A Review of Recent Literature. Prog. Polym. Sci, 2008, 33:399-447. http://dx.doi.org/10.1016/j.progpolymsci.2007.11.001
- [12] Sanchez-polo M., Rivera-utrilla J., Adsorbent-adsorbate interactions in the adsorption of Cd(II) and Hg(II) on ozonised activated carbons, Environ. Sci. Technol., 2002, 36:3850–3854. https://doi.org/10.1021/es0255610.
- [13] Channarong B., Lee S.H., Bade R., Shipin O.V., Simultaneous removal of nickel and zinc from aqueous solution by micellarenhanced ultrafiltration and activated carbon fiber hybrid process, Desalination, 2010, 262:221–227. https://doi.org/10.1016/j.desal.2010.06.016.
- [14] Wang S., Zhu Z.H., Characterisation and environmental application of an Australian natural zeolite for basic dye removal from aqueous solution, J. Hazard. Mater., 2006, 136:946–952. DOI: 10.1016/j.jhazmat.2006.01.038
- [15] Zhang S.Q., Hou W.G., Sorption Removal of Pb(II) from Solution by Uncalcined and Calcined MgAl-Layered Double Hydroxides, Chinese J. Chem., 2007,25:1455-1460. <u>DOI:</u> 10.1002/cjoc.200790269
- [16] Gemeay A.H., El-Sherbiny A.S., Zaki A.B., Adsorption and Kinetic Studies of the Intercalation of Some Organic Compounds onto Na+-Montmorillonite, J. Colloid Interface Sci., 2002, 245:116–125. doi:10.1006/jcis.2001.7989.
- [17] Bulut E., Özacar M., Şengil İ.A, Equilibrium and kinetic data and process design for adsorption of Congo Red onto bentonit, J. Hazard. Mater., 2008, 154:613–622. <u>DOI:</u> 10.1016/j.jhazmat.2007.10.071
- [18] Doğan M., Karaoğlu M.H., Alkan M., Adsorption kinetics of maxilon yellow 4GL and maxilon red GRL dyes on kaolinite J. Hazard. Mater., 2009, 165:1142–1151. https://doi.org/10.1016/j.jhazmat.2008.10.101
- [19] Brigattia M.F., Galan E., Theng B.K.G., Structure and Mineralogy of Clay Minerals, Handbook of Clay Science, 2013, 5:21-81. <u>DOI:</u> 10.1016/B978-0-08-098258-8.00002-X.
- [20] Ahrouch M., Gatica J.M., Draoui K., Vidal H., Adding value to natural clays as low-cost adsorbents of methylene blue in polluted water through honeycomb monoliths manufacture. SN Appl. Sci., 2019, 1:1595. DOI: 10.1007/s42452-019-1636-4.
- [21] Tsai W.T., Chang C.Y., Ing C.H., Chang C.F., Adsorption of acid dyes from aqueous solution on activated bleaching earth, J. Colloid Interface Sci., 2004, 275:72–78. DOI: 10.1016/j.jcis.2004.01.072
- [22] Appel C., Ma L., Rhue, R., Kennelley E., Point of Zero Charge Determination in Soils and Minerals via Traditional Methods and Detection of Electroacoustic Mobility, Geoderma, 2003, 113:77-93. DOI: 10.1016/S0016-7061(02)00316-6
- [23] Ijagbemi C.O., Baek M.H., Kim D.S., Montmorillonite surface properties and sorption characteristics for heavy metal removal from aqueous solutions. J. Hazard. Mater. 2009, 166:538–546. https://doi.org/10.1016/j.jhazmat.2008.11.085
- [24] Jozja N.,B aillif P., Touray J.C., Pons C.H., Muller F., Burgevin C., mpacts « multi-échelle » d'un échange (Mg,Ca)—Pb et ses conséquences sur l'augmentation de la perméabilité d'une bentonite, CR. Geosci., 2003, 335:729–736. DOI:10.1016/S1631-0713(03)00129-9.
- [25] Chouchane T., Chouchane S., Boukari A., Elimination du manganèse en solution par le kaolin Etude cinétique et thermodynamique. Rev. Energ. Renouvelables. 2013,16:313–335.

- [26] Brown G., Brindley G.W., Crystal structures of clay minerals and their X-ray identification. Mineralogical Society London Monograph. 5, 1980 (Ed.)
- [27] Azejjel H., Del Hoyo Martinez C., Draoui K., Rodríguez-Cruz M.S., Sánchez-Martín M.J., Natural and modified clays from Morocco as sorbents of ionizable herbicides in aqueous mediumDesalination, 2009, 249:1151-1158. DOI: 10.1016/j.desal.2009.02.066.
- [28] Heller-Kallai L., Protonation-deprotonation of dioctahedral smectites, Appl. Clay Sci., 2001, 20:27–38. https://doi.org/10.1016/S0169-1317(01)00038-2
- [29] Vicente-Rodríguez M.A., Suarez M., Bañares-Muñoz M.A., Dios Lopez-Gonzalez J., Comparative FT-IR study of the removal of octahedral cations and structural modifications during acid treatment of several silicates, Spectroc. Acta A, 1996, 52:1685– 1694. https://doi.org/10.1016/S0584-8539(96)01771-0
- [30] Kaufhold S., Hein M., R. Dohrmann, Ufer K., Quantification of the mineralogical composition of clays
- using FTIR spectroscopy Vib. Spectrosc., 2012, 59:29–39. https://doi.org/10.1016/j.vibspec.2011.12.012
- [31] Farmer V.C., Infrared spectra of minerals, London, Mineralogical Society 1974. DOI: https://doi.org/10.1180/minmag.1975.040.309.14
- [32] Krukowski E. G., Goodman A., Rother G., Ilton E.S., Guthrie G., Bodnar R. J., FT-IR study of CO2 interaction with Na+ exchanged montmorillonite, Appl. Clay Sci., 2015,114 :61–68. https://doi.org/10.1016/j.clay.2015.05.005
- [33] Cailere S., Henin S., Rautureau M., Mineralogie des Argiles. I Structure et propriétés physico-chimiques, 1982. Ed. Masson, Paris.
- [34] Azarkan S., Peña A., Draoui K., Ignacio Sainz-Díaz C., Adsorption of two fungicides on natural clays of Morocco, Appl. Clay Sci., 2016,123:37–46. DOI: 10.1016/j.clay.2015.12.036.
- [35] Favero J.S, Parisotto-Peterle J., Weiss-Angeli V., Brandalise R. N., Bonan Gomes L., Bergmann C. P., Dos Santos V. Physical and chemical characterization and method for the decontamination of clays for application in cosmetics, Appl. Clay. Sci., 2016, 124–125:252-259. DOI: 10.1016/j.clay.2016.02.022
- [36] Brunauer S., Emmett P.H., E.Teller, Adsorption of Gases in Multimolecular Layers, J. Am. Chem. Soc. 1938, 60:309–319. https://doi.org/10.1021/ja01269a023
- [37] Rouquerol J., Rouquerol F., Llewellyn P., Maurin G., Sing K.S., Adsorption by powders and porous solids: principles, methodology and applications. Academic press. 2013
- [38] Orsini L., Remy J.C., Utilisation du chlorure de cobaltihexammine pour la détermination simultanée de la capacité d'échange et des bases échangeables des sols. Sci Sol., 1976, 4:269–275.
- [39] Krishnan K.A., Sheela A., Anirudhan T.S., Kinetic and equilibrium modeling of liquid-phase adsorption of lead and lead chelates on activated carbons, J. Chem. Technol. Biotechnol., 2003, 78:642–653. https://doi.org/10.1002/jctb.832
- [40] Lagergren S., Zur theorie der sogenannten adsorption geloster stoffe. K. Sven. Vetenskapsakademiens Handl. 1898, 24:1–39. DOI:10.1007/BF01501332
- [41] Ho Y. S., McKay G., Pseudo-second order model for sorption processes Pseudo Process Biochem., 1999, 34:451-465. https://doi.org/10.1016/S0032-9592(98)00112-5
- [42] Ho Y.S., McKay G., A multi-stage batch sorption design with experimental data, Adsorpt. Sci.Technol., 1999,17:233-243. https://doi.org/10.1177/026361749901700401.
- [43] Salleh M.A.M., Mahmoud D.K., Karim W.A.W.A, Idris A. Cationic and Anionic Dye Adsorption by Agricultural Solid Wastes: A Comprehensive Review, Desalination. 2011, 280:1–13, http://dx.doi.org/10.1016/j.desal.2011.07.019
- [44] Jalil Aishah A. A., Triwahyono S., Adam S. H., Rahim N. D., Aziz M. A. A., Hairom N. H. H., Razali N. A. M., Abidin M. A.Z., Mohamadiah M. K. A., Adsorption of methyl orange from aqueous solution onto calcined Lapindo volcanic mud, J. Hazard. Mater., 2010,181:755–762,
- https://doi.org/10.1016/j.jhazmat.2010.05.078
- [45] Li Q., Yue Q.Y., Su Y., Gao B.-Y., Li J., Two-step kinetic study on the adsorption and desorption of reactive dyes at cationic polymer/bentonite, J. Hazard. Mater., 2009, 165:1170–1178. https://doi.org/10.1016/j.jhazmat.2008.10.110
- [46] Weber W.J., Morris J.C., Advances in water pollution research:

- removal of a biologically resistant pollutant from wastewater by adsorption. International Conference on Water Pollution Symposium. Pergamon, Oxford, 1962, 2:231-266
- [47] Eren E., Investigation of a basic dye removal from aqueous solution onto chemically modified Unye Bentonite, J. Hazard. Mater., 2009, 166:88–93. <u>DOI: 10.1016/j.jhazmat.2008.11.011</u>
- [48] Low M. J. D., Kinetics of Chemisorption of Gases on Solids, Chem. Rev., 1960, 60:267-312. https://doi.org/10.1021/cr60205a003
- [49] Chien S.H., Clayton W.R., Application of Elovich Equation to the Kinetics of Phosphate Release and Sorption in Soils, Soil Sci. Soc. Am. J., 1980, 44:265–268.
- https://doi.org/10.2136/sssaj1980.03615995004400020013x
- [50] Khan M.N., Zareen U., sorption process for the removal of sodium dodecyl sulfate (anionic surfactant) from water, J. Hazard. Mater., 2006,133:269–275. DOI: 10.1016/j.jhazmat.2005.10.031.
- [51] Cao J., Guo H., Zhu H.M., Jiang L., Yang H., Effects of SOM, surfactant and pH on the sorption–desorption and mobility of prometryne in soils, Chemosphere , 2008, 70, 2127–2134. https://doi.org/10.1016/j.chemosphere.2007.08.062
- [52] Yu L., Luo Y., The adsorption mechanism of anionic and cationic dyes by Jerusalem artichoke stalk-based mesoporous activated carbon, J. Environ. Chem. Eng., 2014, 2 :220–229. https://doi.org/10.1016/j.jece.2013.12.016
- [53] Langmuir I., The Constitution and Fundamental Properties of Solids and Liquids. Part I. Solids J. Am. Chem. Soc., 1916, 38:2221–2295. http://dx.doi.org/10.1021/ja02268a002
- [54] Freundlich H., Über die adsorption in lösungen. Z. Für Phys. Chem. 1907, 57:385–470. https://doi.org/10.1515/zpch-1907-5723
- [55] Dabrowski A., Adsorption-From Theory to Practice. Advances in Colloid and Interface Science, Adv. Colloid Interface Sci., 2001,93:135-224. http://dx.doi.org/10.1016/S0001-8686(00)00082-8
- [56] Ozcan A., Oncu E. M., Ozcan A. S., Kinetics, isotherm and thermodynamic studies of adsorption of Acid Blue 193 from aqueous solutions onto natural sepiolite, Colloids Surf. A Physicochem. Eng. Asp. 2006, 277:90–97. https://doi.org/10.1016/j.colsurfa.2005.11.017
- [57] Tuzen M., Sarı A. Biosorption of selenium from aqueous solution by green algae (Cladophora hutchinsiae) biomass: Equilibrium, thermodynamic and kinetic studies, Chem. Eng. J., 2010,158:200– 206
- [58] Temkin M. I., Acta Physiochim. URSS. 1940, 12:327–356. <u>DOI:</u> 10.1016/j.cej.2009.12.041
- [59] Hayward D.O., Trapnell B.M.W. Chemisorption. Butterworths London. 1964
- [60] Rytwo G., Ruiz-Hitzky E., Enthalpies of adsorption of methylene blue and crystal violet to montmorillonite, J. Therm. Anal. Calorim., 2003, 71:751–759. https://doi.org/10.1023/A:1023309806214.